ISSN 0006-2979, Biochemistry (Moscow), 2019, Vol. 84, No. 1, pp. 20-32. © Pleiades Publishing, Ltd., 2019.
Original Russian Text © A. S. Karyagina, T. M. Grunina, A. M. Lyaschuk, E. V. Voronina, R. A. Marigin, S. A. Cherepushkin, I. N. Trusova, A. V. Grishin, M. S. Poponova, P. A. Orlova, V. N. Manskikh, N. V. Strukova, M. S. Generalova, K. E. Nikitin, L. A. Soboleva, I. S. Boksha, A. V. Gromov, 2019, published in Biokhimiya, 2019, Vol. 84, No. 1, pp. 85-99.
Originally published in Biochemistry (Moscow) On-Line Papers in Press, as Manuscript BM18-197, November 12, 2018.

Recombinant Human Erythropoietin Proteins Synthesized in *Escherichia coli* Cells: Effects of Additional Domains on the *in vitro* and *in vivo* Activities

A. S. Karyagina[1,2,3,a]*, T. M. Grunina[1], A. M. Lyaschuk[1], E. V. Voronina[4], R. A. Marigin[4], S. A. Cherepushkin[4], I. N. Trusova[4], A. V. Grishin[1,2], M. S. Poponova[1], P. A. Orlova[1], V. N. Manskikh[1,3], N. V. Strukova[1], M. S. Generalova[1], K. E. Nikitin[1], L. A. Soboleva[1], I. S. Boksha[1,5], and A. V. Gromov[1,b]*

[1]*Gamaleya National Research Center of Epidemiology and Microbiology, Ministry of Healthcare of the Russian Federation, 123098 Moscow, Russia*
[2]*All-Russia Research Institute of Agricultural Biotechnology, 127550 Moscow, Russia*
[3]*Belozersky Institute of Physico-Chemical Biology, Lomonosov Moscow State University, 119992 Moscow, Russia*
[4]*State Research Institute of Genetics and Selection of Industrial Microorganisms, Kurchatov Institute National Research Center, 117545 Moscow, Russia*
[5]*Research Center of Mental Health, 115522 Moscow, Russia*
[a]*e-mail: akaryagina@gmail.com*
[b]*e-mail: alexander.v.gromov@gmail.com*

Received July 10, 2018
Revised September 14, 2018
Accepted September 14, 2018

Abstract—The aim of this work was to compare biological activities of three variants of bacterially expressed human recombinant erythropoietin (EPO) with additional protein domains: 6His-s-tag-EPO protein carrying the s-tag (15-a.a. oligopeptide from bovine pancreatic ribonuclease A) at the *N*-terminus and HBD-EPO and EPO-HBD proteins containing heparin-binding protein domains (HBD) of the bone morphogenetic protein 2 from *Danio rerio* at the *N*- and *C*-termini, respectively. The commercial preparation Epostim (LLC Pharmapark, Russia) produced by synthesis in Chinese hamster ovary cells was used for comparison. The EPO variant with the *C*-terminal HBD domain connected by a rigid linker (EPO-HBD) possesses the best properties as compared to HBD-EPO with the reverse domain arrangement. It was ~13 times more active *in vitro* (i.e., promoted proliferation of human erythroleukemia TF-1 cells) and demonstrated a higher rate of association with the erythropoietin receptor. EPO-HBD also exhibited the greatest binding to the demineralized bone matrix (DBM) and more prolonged release from the DBM among the four proteins studied. Subcutaneous administration of EPO-HBD immobilized on DBM resulted in significantly more pronounced vascularization of surrounding tissues in comparison with the other proteins and DBM alone. Therefore, EPO-HBD displayed better performance with regard to all the investigated parameters than other examined EPO variants, and it seems promising to study the possibility of its medical use.

DOI: 10.1134/S0006297919010036

Keywords: erythropoietin, heparin-binding domain, proliferation of human erythroleukemia TF-1 cells, vascularization of surrounding tissues

The main function of erythropoietin (EPO) is stimulation of erythropoiesis – differentiation of erythrocyte precursors in the bone marrow [1]. EPO also affects wound healing and restoration of damaged neuronal cells. Recently, EPO involvement in bone tissue remodeling has been reported [2-4]. All the studies on the effects of EPO on bone tissue regeneration in mammals have been conducted using recombinant EPO synthesized in eukaryotic

Abbreviations: a.a., amino acid residue; BMP-2, bone morphogenetic protein-2; DBM, demineralized bone matrix; DTT, dithiothreitol; EPO(R), erythropoietin (receptor); HBD, heparin-binding domain; 6His, six histidine amino acid residues; s-tag, 15-a.a. oligopeptide from bovine pancreatic ribonuclease A.

* To whom correspondence should be addressed.

cells [5-12]. At the same time, active human EPO can be synthesized in *Escherichia coli* expression system [13-18]. Bacterially expressed EPO variants can be produced in large quantities; they are more standardized, and their production is cost-effective and less labor-intensive. However, EPO variants produced by microbial synthesis are not glycosylated and, as a consequence, less soluble and prone to aggregation. The molecular mass of these proteins is approximately 1.5-fold lower than that of the glycosylated protein. This results in faster clearance of the bacterially synthesized proteins from the systemic blood circulation. Nevertheless, these problems could be solved in one way or another [13, 14, 16-18]. Since proteins produced in *E. coli* cells demonstrate biological activity [13-18], it seems promising to develop novel approaches for their practical application, in particular, their usage in bone tissue regeneration.

In the majority of studies on the bone tissue repair, EPO was administered systemically by multiple injections; however, local administration demonstrated very good results as well [12]. Systemic administration of large doses of EPO can cause increased hematocrit and blood viscosity in patients, which could lead to the emergence or aggravation of cardiovascular diseases [19] and thromboembolism [20]. Because local administration of EPO involves significantly lower doses of the protein, it might decrease the probability of adverse side effects and is much less labor-intensive and, therefore, seems a very promising approach to the treatment of bone pathologies.

In order to ensure prolonged action of EPO at the site of administration, its local concentration should be sufficient for the manifestation of biological activity. In the case of protein preparations, this can be achieved by introducing additional protein domains to provide protein binding to the corresponding carrier and its gradual release into surrounding tissues. Heparin-binding domain (HBD) from the bone morphogenetic protein 2 (BMP-2) of *Danio rerio* is one of such domains. This positively charged domain is located in the *N*-terminal part of BMP-2. Its elimination or mutation results in the inability of BMP-2 to bind heparin; and its dissociation constant for heparin is 20 nM, as determined with the BIAcore^{TM}2000 biosensor (Pharmacia Biosensor AB, Sweden) [21]. This domain is used for BMP-2 purification on heparin-Sepharose [21, 22]. HBD retains BMP-2 in the bone tissue via non-specific ionic interactions. It is capable of strong binding to the demineralized bone matrix (DBM) that is produced from the bone tissue [21, 23] and widely used as an implant material containing negatively charged glucosamine glycans. HBD from BMP-2 can be fused to EPO thereby forming the two-domain bifunctional protein that exhibits biological functions of EPO, as well as ability to interact with DBM and other heparin-containing matrices. New recombinant variants of EPO can be obtained using genetic and protein engineering methods by cloning and expression of the corresponding synthetic genes in *E. coli* cells.

In our previous studies, we cloned EPO variants modified with additional protein domains and synthesized the corresponding recombinant proteins in *E. coli* cells [17, 18]. In particular, one of these variants carried the s-tag (15-a.a. oligopeptide from bovine pancreatic ribonuclease A) at the *N*-terminus [17]. This protein exhibited the *in vitro* activity in the proliferation test with human erythroleukemia TF-1 cells that was only one order of magnitude lower than the activity of the recombinant epoetin beta (Epostim; LLC Pharmapark, Russia), a glycosylated form of EPO produced in Chinese hamster ovary cells. In another study, HBD-EPO protein was obtained that carried the HBD from BMP-2 at the *N*-terminus [18]. This protein demonstrated *in vitro* activity in the cell test and *in vivo* activity by increasing of number of reticulocytes in the rat blood after subcutaneous injection. Both activities were approximately two orders of magnitude lower than those observed for Epostim. However, HBD-EPO exhibited more pronounced local activity than Epostim by inducing tissue vascularization, when DBM discs loaded with the same doses of these two proteins were implanted subcutaneously, which could be explained by the fact that, unlike Epostim, HBD-EPO was retained by the DBM ensuring its prolonged action at the implantation site [18]. The reduced *in vitro* activity of HBD-EPO was likely due to the destabilization of the EPO domain by the *N*-terminal HBD domain. We suggested that the *in vitro* activity and, as a consequence, other types of biological activity of this EPO variant can be improved using protein engineering methods, such as domain rearrangement and spatial separation of domains by longer and more rigid linkers [24].

Previously, we developed a rather simple *in vivo* test that allows us to evaluate the ability of recombinant EPO variants to cause tissue vascularization upon local implantation [18]. It is our opinion that at the very beginning of protein characterization, this test could replace labor-intensive and lengthy experiments studying the effects of various EPO variants on regeneration of bone tissue defects and should be investigated in a separate study. The possibility of such replacement is determined by a number of features listed below.

In addition to its main erythropoietic function, EPO causes pleiotropic non-hematopoietic effects; in particular, it affects osteogenesis, angiogenesis, and tissue vascularization. These properties of EPO are mediated by its interaction with the heterodimeric EPOR/CD131 receptors on the surface of non-hematopoietic cells [25, 26]. Both angiogenic and osteogenic activities of EPO are realized via the mTOR, JAK2, and PI3K signaling pathways [26, 27].

EPO increases the number of endothelial cell precursors by recruiting them to the site of damage [28]. In addition, EPO positively affects expression of VEGF (the most important angiogenic factor) [29] and BMP-2 (the most important factor of bone growth and regeneration) [2]. Sun et al. demonstrated significant suppression of

angiogenesis induced by EPO following osteoclastogenesis inhibition by bisphosphonates or osteoprotegerin (OPG) [9], which indicated close relations between these processes. Another mechanism of EPO participation in the bone tissue formation is its influence on the EphrinB2/EphB4 signaling pathway responsible for the interaction of osteoblasts and osteoclasts that plays a key role in the remodeling processes, as well as in the late stages of bone tissue restoration [30].

Hence, the processes of regulation of angiogenesis and osteogenesis mediated by EPO are closely related to each other; moreover, both these processes are essential for regeneration of bone tissue. Formation of vessels in the newly formed bone is necessary for its correct development and functioning. The relationship between the EPO-mediated osteogenesis and angiogenesis accompanied by the upregulated expression of VEGF induced by EPO was demonstrated in the work of Holstein et al. [29]. Characterization of angiogenic activity of the EPO variants is important because it (i) provides experimental confirmation that the recombinant EPO variants possess one of the *in vivo* non-hematopoietic activities of EPO and (ii) proves that the studied proteins exhibit activity essential for the bone tissue regeneration.

The aim of our study was to obtain a new recombinant HBD-containing EPO variant by synthesis in *E. coli* cells and to carry out the comparative characteristics of the newly developed human recombinant EPO variant with those of previously produced variants.

MATERIALS AND METHODS

Strain and plasmid. *Escherichia coli* strain M15 [pREP4] (F^- Φ80ΔlacM15, *thi*, lac^-, mtl^-, $recA^+$, Km^R) and plasmid vector pQE6 (Qiagen, USA) were used.

Generation of gene construct encoding EPO-HBD. Fully synthesized *EPO-HBD* gene (Evrogen, Russia) encoding human EPO and HBD from *Danio rerio* BMP-2 connected by a linker was flanked by the NcoI and Kpn2I sites at the 5′- and 3′-ends, respectively. Optimization of the synthetic gene codon composition, correction of the transcribed RNA secondary structure, and calculation of the molecular mass and theoretical isoelectric point (p*I*) of the encoded polypeptide were carried out using standard approaches as described by Karyagina et al. [31]. The *EPO-HBD* gene was inserted into the pQE6 plasmid by the NcoI and Kpn2I sites; the resulting plasmid was used for the transformation of *E. coli* M-15 [pREP4] cells to generate a producer strain for the synthesis of EPO-HBD carrying HBD at the *C*-terminus (Table 1). The calculated molecular weight and p*I* of EPO-HBD protein were 21,736.55 Da and 10.07, respectively.

EPO-HBD purification. Cultivation of transformed *E. coli* cells, their disruption, isolation of inclusion bodies, chromatographic purification of the recombinant protein on WorkBeads 40 S (Bio-Works, Sweden), protein refolding, and column chromatography on heparin-Sepharose CL-6B (Amersham Pharmacia Biotech, Sweden) have been described in detail earlier [18].

EPO-HBD was purified as described below. Washed inclusion bodies (0.18 g) were dissolved in 8 M urea solution in 20 mM Tris-HCl (pH 8.0) and centrifuged at 9000*g* for 30 min. The supernatant was loaded on a column with WorkBeads 40 S resin (5 ml) equilibrated with 8 M urea in 20 mM Tris-HCl (pH 8.0) at a rate of 1 ml/min. The column was washed at a rate of 2 ml/min until the absorption plateau was reached; the proteins were eluted with a linear 0-1 M NaCl concentration gradient in the same buffer (total volume, 50 ml) at the same rate. Protein fractions (2 ml) were collected; fractions corresponding to the maximal absorption at 280 nm were

Table 1. Erythropoietin variants used in the study: protein molecule structure and *in vitro* and *in vivo* activities in various tests

Protein	Structure/protein molecule features	Activity *in vitro*, ng/ml	Affinity to EPOR, ranks	Parameters of association and disassociation with DBM, ranks	Vessel surface area, μm² (lower – upper quartiles, median)
Epostim	glycosylated EPO	0.68	1	2	220-952 (401)
6His-s-tag-EPO	6His-s-tag-DDDDK-EPO	4.34	2	4	419-1264 (744)
EPO-HBD	EPO-$(AP)_8$-HBD	24.15	3	1	876-4410 (2217)
HBD-EPO	HBD-$(GS)_3$-EPO	319.40	4	3	643-1859 (1098)

Note: DDDDK, enterokinase hydrolysis site; $(AP)_8$, alanine-proline linker; $(GS)_3$, glycine-serine linker; EPOR, erythropoietin receptor. Activity *in vitro* was determined in the proliferation assay with human erythroleukemia TF-1 cell line; affinity to EPOR was determined using the biolayer interferometry method; parameters of association and dissociation with DBM were examined in the experiments on the dissociation kinetics of the EPO variants from DBM; degree of vascularization was estimated from the vessels surface area in histological sections in the experiments on the local angiogenic activity of EPO variants after subcutaneous implantation of DBM discs with applied proteins (see "Materials and Methods" section) into rats. Lower/upper quartiles and median of the vessel surface area in the DBM (control) group were 209-742 and 459 μm², respectively. In the comparative tests, protein demonstrating the highest activity were assigned the rank 1, and the lowest – rank 4.

assayed for the protein concentration and analyzed by PAGE.

Protein fractions after chromatography on WorkBeads 40 S were diluted with 20 mM Tris-HCl (pH 8.0) containing 6 M guanidine hydrochloride and 0.1 M dithiothreitol (DTT) to a final protein concentration ~0.1 mg/ml and incubated for 24 h at 4°C to initiate refolding. Next, the denatured protein solution was dialyzed against 10 volumes of 20 mM Tris-HCl (pH 8.0) containing 1 M guanidine hydrochloride for 24 h (the dialysis buffer was changed three times) and then centrifuged for 30 min at 9000*g*. The supernatant was diluted with the refolding buffer containing 1 M L-arginine in 20 mM Tris-HCl (pH 8.5) at a 1 : 1 ratio (final protein concentration, ~0.05 mg/ml) and incubated for 24 h at 4°C. The refolded protein was dialyzed against 10 volumes of 20 mM Tris-HCl (pH 6.8) containing 4 M urea for 24 h and then centrifuged for 30 min at 9000*g*.

After dialysis, the obtained protein solution was applied on a column with 5 ml of heparin-Sepharose CL-6B equilibrated with 4 M urea in 20 mM Tris-HCl (pH 6.8); the column was washed with the same buffer; all operations were conducted at a flow rate of 1 ml/min. Proteins were eluted with 50 ml of 0-1 M NaCl concentration gradient in 4 M urea solution in 20 mM Tris-HCl (pH 6.8) at a rate of 1 ml/min. Four 2-ml fractions were collected and analyzed by PAGE under nonreducing conditions to estimate the degree of protein aggregation. The protein monomer was detected in the first three fractions; the last fraction contained a small amount of aggregates, as can be seen in the electrophoregrams. The three fractions with a total volume of 6 ml were combined and dialyzed against 10 volumes of 20 mM ammonium acetate (pH 4.5) for 24 h at 4°C with three buffer changes. The concentration of the obtained EPO-HBD was 0.141 mg/ml. The protein was lyophilized and used for further investigations (dried protein preparations were highly soluble in physiological saline).

Evaluation of *in vitro* biological activity of proteins in proliferation assay with human erythroleukemia TF-1 cells. Biological activity of the EPO preparations was examined *in vitro* in the proliferation assay with the human erythroleukemia TF-1 cell line (ATCC CRL-2003) according to the protocol described in European Pharmacopoeia, 9th edition, as described in the paper of Grunina et al. [17].

Estimation of the protein binding efficiency with the recombinant human EPOR using biolayer interferometry technique. The binding kinetics of the investigated proteins with human EPOR/Fc receptor (SinoBiological, China) immobilized on the surface of a Protein A biosensor was studied by the biolayer interferometry technique in a real-time mode using an Octet K2 system (Fortebio/Pall, USA) [32].

A 96-well interferometry plate contained human EPOR/Fc receptor at a concentration of 0.5 μg/ml and aliquots of each investigated protein (20 nM) in 1× buffer for association kinetics assay recommended by the manufacturer (Fortebio, USA). The time for the receptor immobilization was programmed with the function threshold 0.85 nm. The duration of the association and dissociation steps was set at 600 s. Analysis was carried out at 30°C and mixing rate of 1000 rpm. The buffer for association kinetics assay mentioned above was used as a negative control. For each of the investigated samples, individual fiber optic Protein A biosensor paired with the control sensor were used to monitor protein association.

Statistical processing of the obtained results was carried out with the Fortebio Data Analysis 9.0 software (Fortebio, USA).

Kinetics of the release of EPO variants from DBM. DBM membranes (thickness, 3-4 mm) were produced from a bovine femur bone diaphysis according to the previously developed method [33] with slight modifications [23]. The discs (4 mm in diameter) were cut from the membranes; discs weighing 10 ± 1 mg were used to apply the proteins.

For protein immobilization, each disc was placed in 100 μl of solution containing 10 μg of protein in 25 mM sodium phosphate buffer (pH 5.5) and incubated with shaking in an orbital shaker S-3 (Elmi Ltd., Latvia) at a speed of 10 rpm and a platform angle of 5° for 5 h under vacuum, followed by washing with 1 ml of the same buffer for 20 min repeated three times. Next, the discs were frozen and lyophilized.

To examine protein release, lyophilized discs with applied proteins were placed into polypropylene tubes with caps; 1 ml of incubation buffer containing 25 mM sodium phosphate (pH 5.5), 1% BSA, and 0.2% sodium azide was added to each tube. The tubes were incubated at room temperature with shaking at 300 rpm. The entire sample volume was removed after 1, 5, 24, and 48 h and 3, 7, 14, 21, and 28 days and replaced each time with 1 ml of the incubation buffer. The collected samples were frozen. On completion of the experiment, protein concentration in the samples was measured by the previously developed ELISA procedure [18].

Evaluation of local angiogenic activity of proteins. Local angiogenic activity of EPO variants was estimated using subcutaneous implantation of DBM fragments with applied proteins followed by histological evaluation of the degree of vascularization of adjacent tissues according to the technique described by Karyagina et al. [18] with minor modifications. In short, 15 Sprague–Dawley male rats (body weight, 270-280 g) were separated into five groups with 3 individuals in each. Two DBM discs loaded with the same protein were implanted subcutaneously into each rat under anesthesia into the temple regions symmetrically on both sides of the head. Four test groups were implanted with DBM discs loaded with 1 μg of HBD-EPO, EPO-HBD, 6His-s-tag-EPO, or Epostim,

and the fifth group – with empty DBM discs. One day before the surgery, the discs were placed into 1.5-ml plastic tubes with caps, and 20 μl of 25 mM phosphate buffer (pH 5.5) containing 1 μg of the tested protein was applied onto them followed by overnight incubation at 10°C; the discs were then used for implantation without prior lyophilization.

After 5 days, the animals were euthanized by carbon dioxide inhalation, and the discs were removed together with the adjacent tissues. Sections (4 μm thick) from the formalin-fixed and paraffin-embedded discs were stained with hematoxylin-eosin or azan according to Heidenhain [34] followed by histological analysis. The degree of vascularization was estimated by performing quantitative comparative analysis of the surface area of vessels in the sections. Statistical analysis was carried out using the Kruskal–Wallis criterion ($p < 0.01$) with the Statistica 12.0 software (Statsoft, USA).

RESULTS

The two-domain recombinant EPO-HBD protein consisting of the human EPO amino acid sequence, linker, and the HBD from *D. rerio* BMP-2 was produced as described in "Materials and Methods". Schematic representation of the structures of previously produced proteins HBD-EPO [18] and 6His-s-tag-EPO [16] used for comparative examination, as well as of EPO-HBD obtained in this work, is shown in Table 1.

EPO-HBD was purified by the method very similar to the procedure previously developed for the purification of HBD-EPO [18]. The total amount of the purified EPO-HBD was 0.85 mg. The data on the purification efficiency and EPO-HBD yield are presented in Table 2.

The electrophoregram of the purified 6His-s-tag-EPO, HBD-EPO, and EPO-HBD proteins under reducing and nonreducing conditions in 12% polyacrylamide gel is shown in Fig. 1. The proteins were electrophoretically homogenous; neither high molecular weight aggregates, nor low molecular weight proteins were detected in the preparations. The electrophoretic mobility of all three proteins under nonreducing conditions (Fig. 1, lanes *1*, *3*, *5*) was higher in comparison with the mobility under reducing conditions (in the presence of DTT) (Fig. 1, lanes *2*, *4*, *6*).

Table 2. EPO-HBD yield in the process of its purification

Purification stage	Amount of protein, mg per g wet biomass	HBD-EPO content, %
Biomass (after gene expression induction)	23.8	42.7
Inclusion bodies	18.3	90.2
Chromatography on WorkBeads 40 S	5.4	95.3
Refolding and chromatography on heparin-Sepharose CL-6B	0.85	99.5

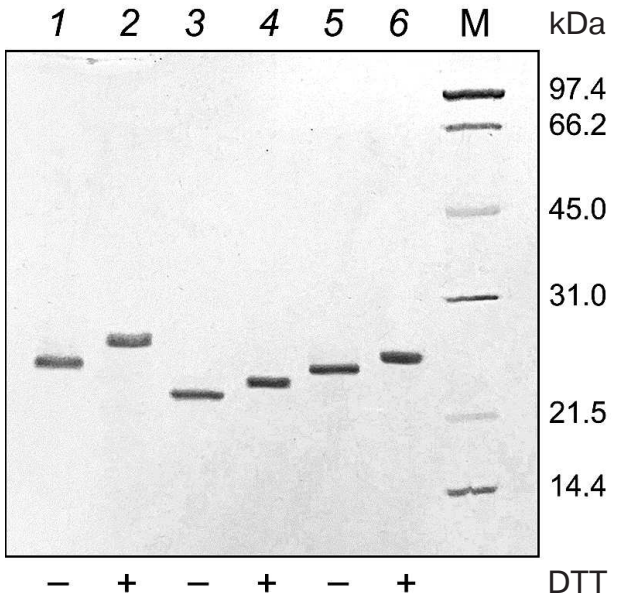

Fig. 1. Electrophoregram in 12% polyacrylamide gel of purified 6His-s-tag-EPO (lanes *1* and *2*; calculated molecular mass 23.8 kDa), HBD-EPO (lanes *3* and *4*; calculated molecular mass 20.5 kDa), and EPO-HBD (lanes *5* and *6*; calculated molecular mass 21.7 kDa); *1*, *3*, *5* – nonreducing conditions; *2*, *4*, *6* – reducing conditions; M (14-97 kDa), protein molecular weight markers (Bio-Rad, USA). All protein preparations were treated with the sample buffer with or without DTT prior to loading onto a gel. Presence (+) or absence (–) of DTT in the sample buffer is shown under the respective lanes.

The *in vitro* activities of the purified EPO-HBD, 6His-s-tag-EPO, HBD-EPO, and Epostim obtained by synthesis in eukaryotic cells were measured in the test with human erythroleukemia TF-1 cells (Fig. 2).

The EC_{50} value for the eukaryotic Epostim was 0.68 ng/ml (mean value from three replicates); the EC_{50} values for the prokaryotic 6His-s-tag-EPO, EPO-HBD, and HBD-EPO were 4.34, 24.15, and 319.40 ng/ml, respectively (Table 1).

The results on *in vitro* activity assay with the erythroleukemia cells were corroborated by the biolayer interferometry used to estimate the relative affinity of the investigated EPO variants to EPOR (EPO receptor) (Fig. 3).

According to the decrease in the association rate with EPOR, the proteins were arranged in the following order: Epostim (the highest association rate) → 6His-s-

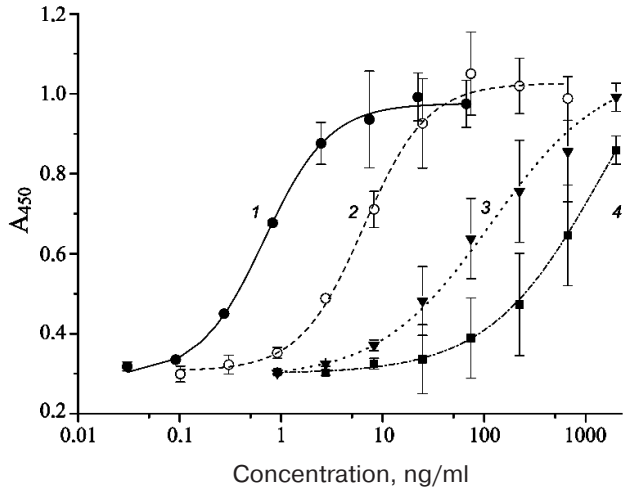

Fig. 2. Dependencies of the optical density in the well on the sample concentration in the *in vitro* activity assay of different EPO variants with human erythroleukemia TF-1 cells: *1*) Epostim; *2*) 6His-s-tag-EPO; *3*) EPO-HBD; *4*) HBD-EPO. Bars, standard deviation (all measurements were done in triplicate).

tag-EPO → EPO-HBD → HBD-EPO. The lower speed of the association corresponds to the lower slope of the curve in the first part of the interferometric profile (Fig. 3). For the sake of convenience, the data on the affinity of different EPO variants to EPOR are presented in Table 1 as ranks, with rank 1 assigned to Epostim demonstrating the highest affinity and rank 4 assigned to HBD-EPO exhibiting the lowest affinity.

It also seemed interesting to estimate the ability of these proteins to bind to and to dissociate from the carrier (DBM), which assumingly correlates with the presence and integrity of HBDs in these proteins. In order to evaluate the binding of EPO variants to the DBM, we studied the dissociation kinetics of these proteins from the DBM discs. Protein aliquots (10 μg) were applied onto the discs (disk weight, 10 ± 1 mg) and lyophilized as described in "Materials and Methods". The discs with applied proteins were incubated in 1 ml of the incubation buffer, the entire volume of which was replaced with a new portion after 1, 5, and 24 h, and after 2, 3, 7, 14, 21, and 28 days. The amount of the released protein was determined by sandwich ELISA. The cumulative curves of protein release during the first three days are presented in Fig. 4. The protein ranking according to the efficiency of their binding to DBM is presented in Table 1, with the most efficient binding ranked as 1, and the least efficient binding ranked as 4.

As seen from Fig. 4, the maximum amount of protein associated with DBM was found for EPO-HBD. The gradual release of EPO-HBD from the carrier (on average, 30 ng protein per day) within 5 to 72 h was approximately 3-fold higher than for all other proteins, as manifested by a noticeably higher slope of the EPO-HBD curve during this time period in comparison with the other curves. Between the days 21 and 28, EPO-HBD

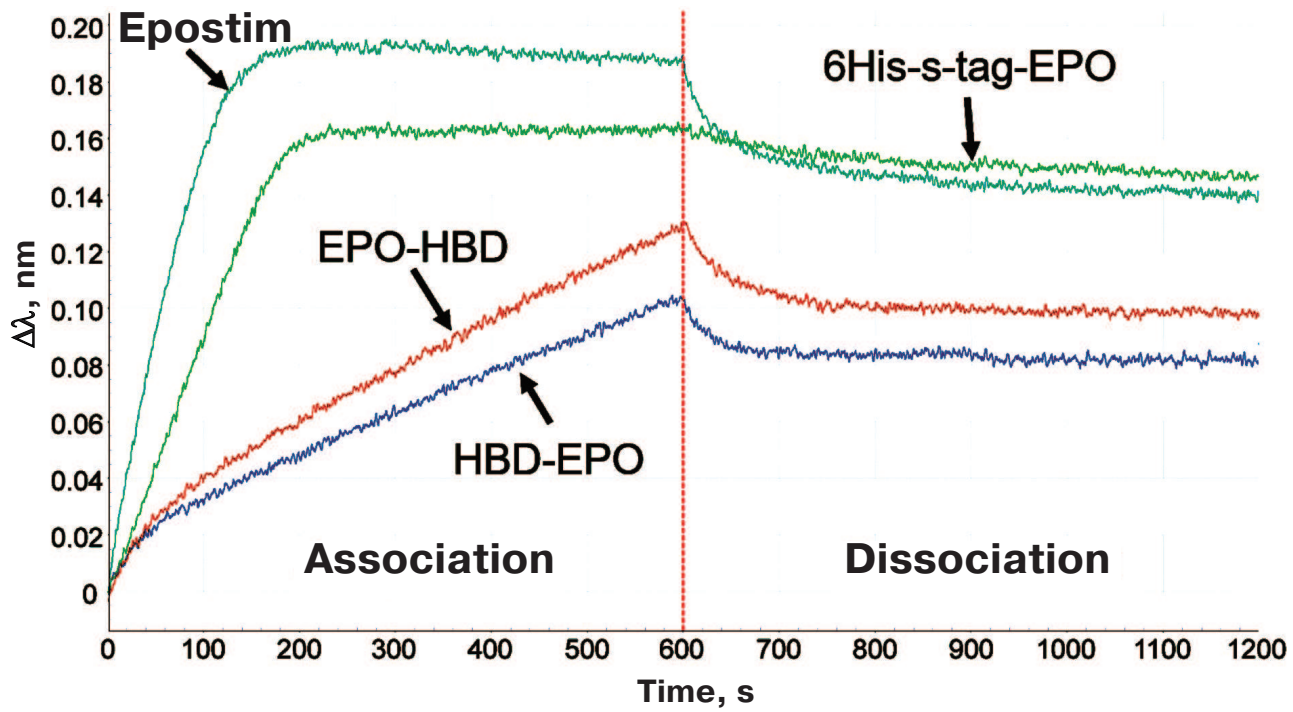

Fig. 3. Interferometric profiles of the association/dissociation of the investigated 6His-s-tag-EPO, HBD-EPO, EPO-HBD proteins and Epostim in solution with the human EPOR/Fc receptor immobilized on Protein A biosensor.

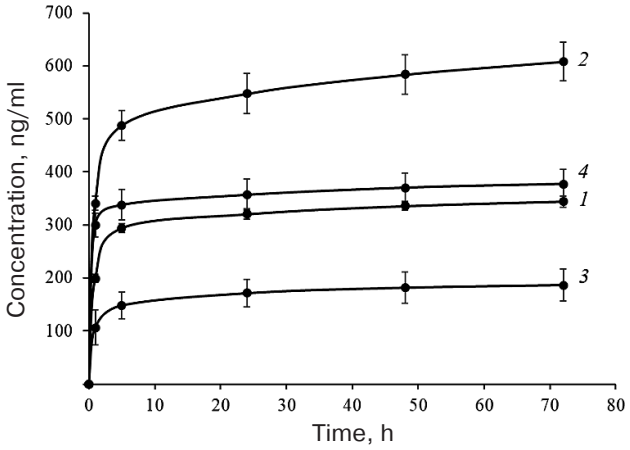

Fig. 4. Cumulative dissociation curves of the investigated EPO variants from DBM discs: *1*) HBD-EPO; *2*) EPO-HBD; *3*) 6His-s-tag-EPO; *4*) Epostim. Three DBM discs were analyzed for each protein. Circles and upper and lower error bars correspond to mean value and standard deviation, respectively. Protein concentration in the samples was measured with the previously developed ELISA test system [18].

could be detected by ELISA, which corresponded to the release of 1.5 ng protein per day; the amounts of 6His-s-tag-EPO, HBD-EPO, and Epostim were below the ELISA detection limits. The lowest association and the lowest release from DBM were observed for 6-His-s-tag-EPO that lacks the HBD.

In order to compare the *in vivo* activity of the EPO variants, we analyzed their ability to induce vascularization of surrounding tissues after subcutaneous implantation of DBM discs loaded with the tested proteins (1 μg protein per disc) followed by histological examination. Empty DBM discs were used as a control. The discs were removed together with surrounding tissues 5 days after the implantation and stained with hematoxylin-eosin (for histological evaluation of the image) and azan (for quantification of the vessel surface) [34].

The histological pattern was found to be very similar in all the groups. Epidermis, dermis, and their appendages were intact in all samples. The implants were located in the adventitia as fragments of decellularized trabecular bone without any signs of osteoclast resorption or perifocal osteogenesis. The space between the trabeculae was filled with poorly organized fibrin with a small number of cellular elements (leucocytes and macrophages). Low or moderate inflammation was detected on the periphery of the transplantation site accompanied by formation of mature granulation tissue from the fibroblast-like elements and macrophages and weak or moderate infiltration of lymphocytes and plasma cells.

The main difference between the tested proteins was in the extent of tissue vascularization (Fig. 5 and Table 1). Lower and upper quartiles, as well as the median values, for the vessel surface area in μm^2 are presented in Table 1. The lowest degree of vascularization was observed in the control group (empty DBM discs) and in the case of DBM discs with Epostim. Small erythrocyte-containing vessels with the surface area of 209-742 μm^2 (median 459 μm^2) (control DBM discs) and 220-952 μm^2 (median 401 μm^2) (DBM discs with Epostim) were mostly concentrated on the implantation site periphery along the subcutaneous muscle layer. Similar pattern with slightly more pronounced vascularization including a larger number of vessels with larger surface area was observed in the case of implantation of DBM discs loaded with 6His-s-tag-EPO (419-1264 μm^2, median 744 μm^2). The most pronounced vascularization pattern was observed for HBD-EPO and EPO-HBD. The vessels of various sizes, from small to very large, with the surface area of 643-1859 μm^2, median 1098 μm^2 in the case of HBD-EPO and 876-4410 μm^2, median 2217 μm^2 in the case of EPO-HBD were observed both on the periphery and in the tissues located closer to the center of the implantation site.

Statistical analysis of the vessel surface area in the histological sections of samples with implanted DBM + HBD-EPO and DBM + EPO-HBD demonstrated statistically significant differences as compared with the control group (DBM) and the DBM + Epostim group (Fig. 6). By the area of vessels, the DBM + 6His-s-tag-EPO group showed the significant difference only with the DBM + EPO-HBD, but not with DBM + HBD-EPO.

Most of the results obtained in the study are summarized in Table 1.

DISCUSSION

In the previous study [18], we constructed a recombinant EPO variant containing an additional HBD domain from *D. rerio* BMP-2 and synthesized it in *E. coli* cells. The HBD provided binding of the recombinant protein with heparin-containing substrates and matrices, e.g., DBM, which is commonly used as an implantable material for bone tissue repair. HBD-EPO exhibited *in vitro* biological activity, including the ability to promote proliferation of human erythroleukemia TF-1 cells. This activity was by two orders of magnitude lower than the activity of eukaryotically synthesized Epostim. At the same time, the local *in vivo* activity manifested as vascularization of surrounding tissues 5 days after subcutaneous implantation of DBM with applied EPO variant (1 μg) was significantly higher for HBD-EPO than for Epostim. This effect might be explained by more prolonged action of HBD-EPO: unlike Epostim, HBD-EPO possesses HBD, which provides binding and retention of HBD-EPO on DBM. The fact that such a low dose of HBD-EPO (1 μg) [18] induces highly pronounced tissue vascularization within a short period of time (5 days) indicates that this EPO variant offers promise for application in

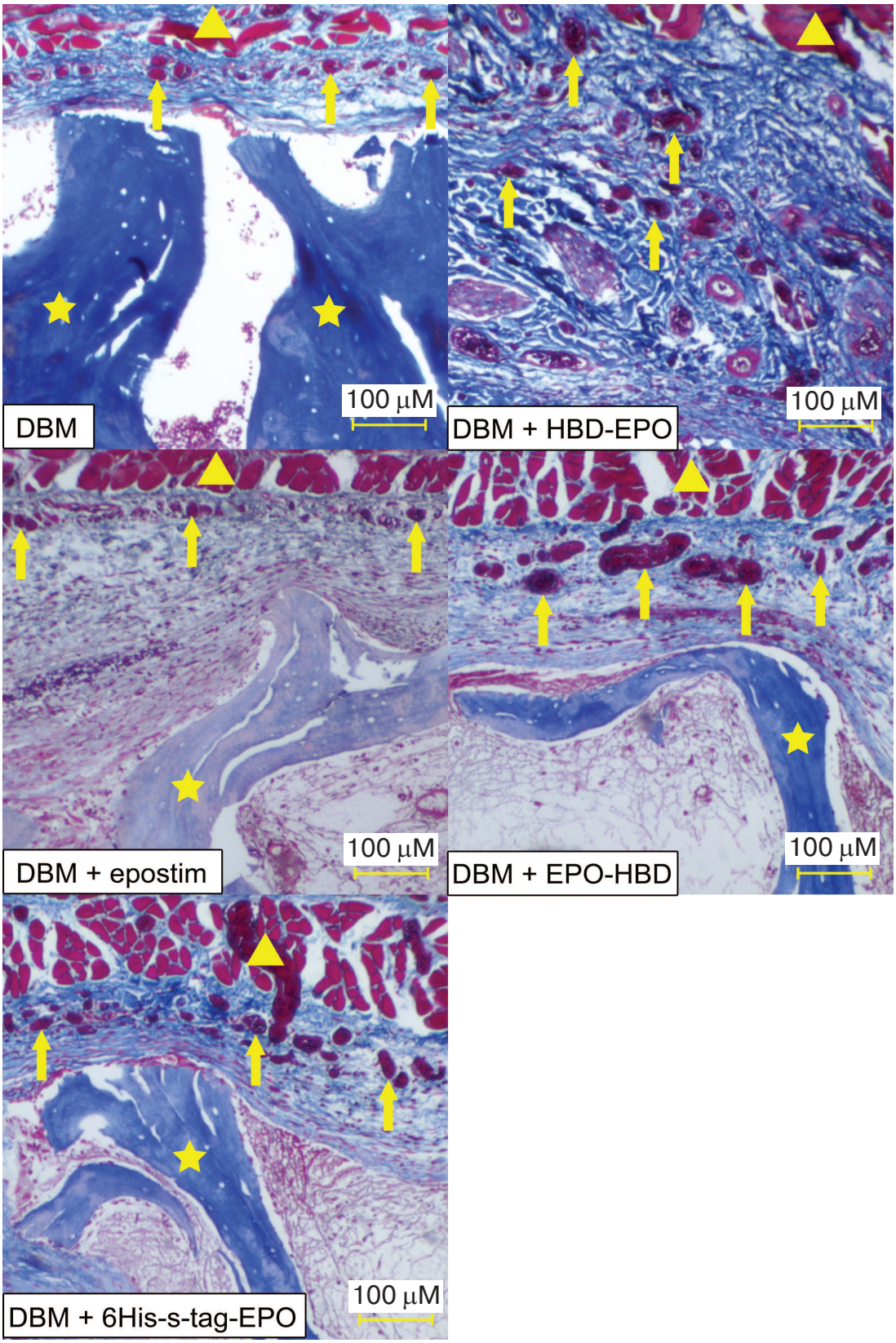

Fig. 5. Microscopic image of the tissue samples from the sites of subcutaneous implantation of DBM discs without and with the applied proteins 5 days after implantation (azan staining according to Heidenhain [34]). Magnification, 40×. Triangles, subcutaneous muscle fibers; arrows, vessels filled with azan-stained red erythrocytes; asterisks, fragments of DBM implants representing decellularized trabecular bones.

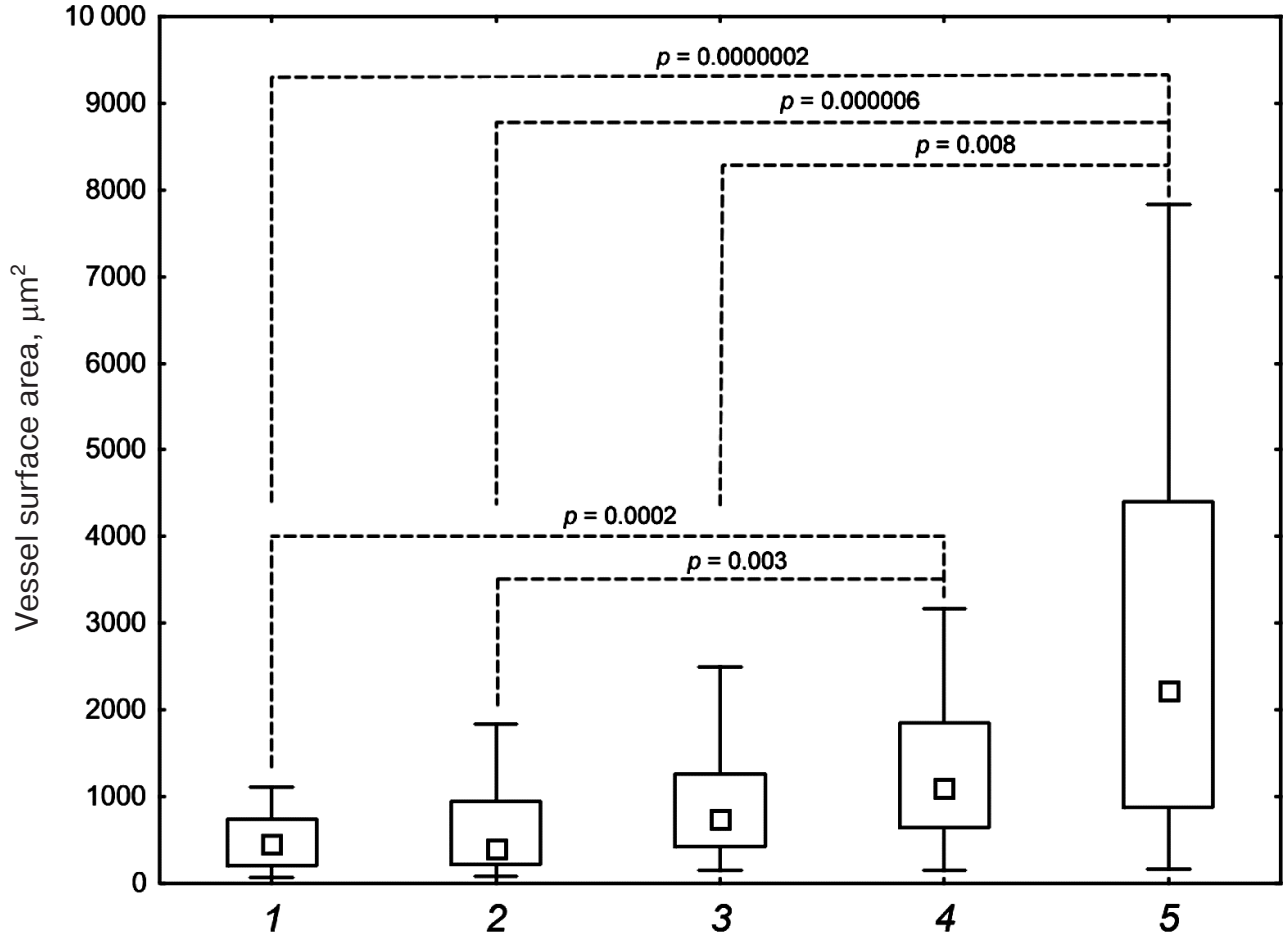

Fig. 6. Vessel surface area in histological sections after subcutaneous implantation of DBM disks: *1*) DBM; *2*) DBM + Epostim; *3*) DBM + 6His-s-tag-EPO; *4*) DBM + HBD-EPO; *5*) DBM + EPO-HBD. Small squares, median values; rectangle boundaries, lower and upper quartiles, bars, value range values; dashed lines, *p* values for the group comparison obtained using the Kruskal–Wallis criterion.

regenerative medicine. Nevertheless, it still can be possible to improve protein properties using protein engineering.

The recombinant HBD-EPO protein constructed in [18] contains HBD domain at the *N*-terminus of the molecule. We have selected this placement of HBD based on its location in the natural BMP-2 molecule in all animal species. At the same time, the *N*-terminal placement of HBD could interfere with the chromatographic separation of the full-length protein from proteins with truncated polypeptide chain if heparin-Sepharose is used for purification [18], which could reduce the yield of the target protein due to the necessity to discard fractions containing its truncated variants. Hence, we decided to place the HBD domain at the *C*-terminus to generate a new variant of recombinant EPO. In order to avoid interference of protein domains, it is recommended to use linkers with enhanced rigidity that contain proline residues alternating with other amino acids [24]. During the design of the novel recombinant EPO-HBD protein, we used long rigid linker NH_2-GSPAPAPAPAPAPAPA-PARS-COOH instead of the flexible NH_2-GSGSGS-COOH linker used before for connecting domains in HBD-EPO. The structures of EPO-HBD and previously produced HBD-EPO and 6His-s-tag-EPO are schematically shown in Table 1.

Purified 6His-s-tag-EPO, HBD-EPO, and EPO-HBD demonstrated different electrophoretic mobilities according to the differences in their molecular masses (Fig. 1). Protein purification by chromatography on WorkBeads 40 S, refolding, and following chromatography on heparin-Sepharose CL-6B produced the oxidized forms of these proteins (see "Materials and Methods"). Oxidized 6His-s-tag-EPO and HBD-EPO have the structure close to the native one with two S–S-bonds formed by four cysteine residues, as has been shown previously by mass spectrometry [17, 18]. The electrophoretic mobility of the oxidized forms of all three proteins (Fig. 1, lanes *1*, *3*, and *5*) is higher than the mobility of the reduced forms in the presence of DTT (Fig. 1, lanes *2*, *4*, and *6*). EPO-

HBD was purified and refolded under the same conditions as HBD-EPO [18]. The oxidized and reduced forms of EPO-HBD demonstrated mobilities that were in between the mobilities of the respective forms of 6His-s-tag-EPO and HBD-EPO, which is in agreement with their molecular masses. This suggests that both intramolecular disulfide bonds characteristic for EPO were also likely present in the oxidized form of EPO-HBD.

The results of the *in vitro* activity assay using human erythroleukemia TF-1 cells revealed that the specific activities of 6His-s-tag-EPO, EPO-HBD, and HBD-EPO comprised 15.6, 2.8, and 0.2%, respectively, of the activity of Epostim. Hence, domain rearrangements and replacement of the linker with a more rigid and longer one in EPO-HBD increased its activity by more than one order of magnitude (13-fold) compared to HBD-EPO. The activity of 6His-s-tag-EPO was higher than those of both HBD-modified EPO variants and corresponded to the previously determined activity of this protein (13.4%) [17].

The biolayer interferometry method based on the phenomenon of light interference was used to investigate interactions of all EPO variants with EPOR. The incoming beam of the white light is reflected from the surface of a fiber optic biosensor with the applied layer of biocompatible protein A. Sequential high-affinity interaction of the protein A-coated biosensor with the Fc-fragment of the receptor, and then interaction of the receptor with the tested EPO variants produced interferometric profiles in real-time. Using this method, we found that Epostim demonstrated the highest association rate with EPOR among the four investigated proteins (Fig. 3). 6His-s-tag-EPO also exhibited high association rate with EPOR, although it was lower than for Epostim. Interestingly, the dissociation rate for 6His-s-tag-EPO was lower than for Epostim (Fig. 3). EPO-HBD and HBD-EPO demonstrated low rates of association with EPOR in comparison to 6His-s-tag-EPO and Epostim. The lowest association rate was observed for HBD-EPO.

The interferometric profiles for EPO-HBD and HBD-EPO were non-linear in the time range from 0 to 100 s (Fig. 3). This indicates that these preparations likely contained a fraction with different affinity to the receptor, which became clearly visible with the increase in the protein concentration to >20 nM (data not shown). The observed heterogeneity was probably related to the presence of certain amounts of high molecular weight aggregates that could not be identified electrophoretically or forms with incorrectly formed disulfide bonds that had lower affinity to the receptor. We assume that the heterogeneity of the preparations could also affect their *in vitro* activity.

Thus, according to the results of the *in vitro* proliferation activity assay and analysis of the affinity to the EPOR, the tested EPO variants can be arranged in the following order of decreasing activity: Epostim → 6His-s-tag-EPO → EPO-HBD → HBD-EPO (Table 1).

The results of experimental evaluation of the ability of the investigated proteins for association and retention on the DBM carrier are in general agreement with the presence and intactness of the HBD domain in them. The highest association was demonstrated for EPO-HBD carrying the HBD at the *C*-terminus that was separated from the EPO domain with the rigid linker, and the lowest – for 6His-s-tag-EPO lacking the HBD (Fig. 4 and Table 1).

Interestingly, Epostim, which does not have the HBD, has nevertheless demonstrated even slightly better binding and dissociation from the DBM than HBD-EPO that differed from EPO-HBD (which exhibited the highest binding to DBM) by the domain rearrangement and different linker. This ability of Epostim can be likely explained by its glycosylation, which facilitates interaction with the DBM despite the presence of negatively charged sialic acids at the ends of the carbohydrate chains.

Hence, the placement of HBD at the *C*-terminus in EPO-HBD not only improved protein *in vitro* proliferative action on cells and increased its association rate with EPOR, but also significantly promoted its association with DBM, prolonged the release time, and increased the amount of released protein in comparison to HBD-EPO and other proteins. Such effect was probably due to more suitable mutual arrangement of the domains and decrease of their interactions due to the use of more rigid linker.

The *in vivo* activity of the tested EPO variants manifested as vascularization of the surrounding tissues was compared. Tissue samples stained with hematoxylin-eosin (for evaluation of general histological pattern) and azan [34] (for quantification of vessel surface area) were studied. Azan staining facilitates visualization of vessels containing erythrocytes and has been used in other studies, e.g., for estimation of tissue vascularization after combined action of the recombinant SDF-1a and BMP-2 factors on regenerating bone tissue [35] instead of traditional immunohistochemical approach employing CD31 antibodies as endothelial cell markers. Earlier, we used azan staining for quantification of vessels containing erythrocytes to evaluate the degree of vascularization of surrounding tissues after subcutaneous introduction of DBM implants loaded with HBD-EPO and Epostim [18]. Here, we conducted an extended experiment using the same technique, but adding 6His-s-tag-EPO and EPO-HBD to the tested proteins, as well as using empty DBM for comparison.

The obtained data (Figs. 5 and 6) are in a good agreement with the theoretical notion that the best ability to cause vascularization of surrounding tissues during implantation of DBM discs should be demonstrated by proteins retained on the discs due to the presence of HBD (EPO-HBD and HBD-EPO) and, hence, creating higher local concentration of the factors inducing angiogenesis and vascularization at the site of implantation.

In our opinion, further evaluation of possible medical applications of the produced EPO variants with additional protein domains, especially of EPO-HBD, may be

of significant interest. Nevertheless, the question on possible immunogenicity of the two-domain protein of prokaryotic origin upon its introduction into the human organism remains open, since the safety of a particular implantable material can be evaluated only in pre-clinical and clinical trials. However, it should be mentioned that the generated EPO variants are intended not for systemic application but rather for local introduction into the bone tissue. Modern surgical techniques can prevent implantable materials from entering the blood and adjacent tissues, which should significantly limit the development of adverse immune response. So far, there are no data available on the development of immune response during local implantation of recombinant EPO preparations of prokaryotic origin. However, numerous studies on the immune response in patients after local introduction of the INFUSE® Bone Graft (Medtronic, USA) for bone tissue regeneration have been published. INFUSE® Bone Graft is a collagen sponge loaded with the recombinant rhBMP-2 (lyophilized rhBMP-2 is dissolved in distilled water and applied to the sponge immediately prior to the implantation into the bone defect site). These data indicate low immunogenicity of rhBMP-2 and the absence of correlation between the development of complications after of INFUSE®Bone Graft application and the presence of antibodies against rhBMP-2 in the patients' blood [36].

In conclusion, we have demonstrated that the placement of HBD domain at the *C*-terminus of EPO and the use of a more rigid proline-alanine linker allows production of active recombinant EPO-HBD via synthesis in *E. coli* cells. The obtained protein demonstrates ~13-fold higher *in vitro* activity in the proliferation test with human erythroleukemia TF-1 cells than HBD-EPO. EPO-HBD also exhibits higher association rate with EPOR in comparison to HBD-EPO, as has been shown in experiments using biolayer interferometry. EPO-HBD exhibits the best parameters for binding to DBM and gradual release from the matrix among all other investigated proteins (Epostim, HDB-EPO, and 6His-s-tag-EPO). Moreover, EPO-HBD shows the maximal ability to stimulate tissue vascularization after subcutaneous implantation while loaded on DBM. All the above-mentioned features suggest that the newly designed recombinant EPO variant, EPO-HBD, can be further investigated for its possible medical application, e.g., in the experiments on bone tissue regeneration, either by itself or in combination with other protein factors, such as BMP-2, which will be the subject of our future studies.

Funding

This work was financially supported by the Russian Science Foundation (project no. 16-15-00133).

Acknowledgements

Authors are grateful to Z. M. Galushkina for providing cell biomass for protein purification and M. S. Krivozubov for help in preparation of DBM discs.

Conflict of Interest

Authors declare no conflict of interest in financial or any other sphere.

Ethics Committee Approval

All procedures involving animals performed in the investigation were in compliance with the "Rules of conducting experiments with participation of laboratory animals" of the Gamaleya National Research Center of Epidemiology and Microbiology, Ministry of Healthcare of the Russian Federation, and the EU Directive 2010/63/EU and Appendix A of European Convention ETS no. 123.

REFERENCES

1. Krantz, S. B. (1991) Erythropoietin, *Blood*, **77**, 419-434.
2. Shiozawa, Y., Jung, Y., Ziegler, A. M., Pedersen, E. A., Wang, J., Wang, Z., Song, J., Wang, J., Lee, C. H., Sud, S., Pienta, K. J., Krebsbach, P. H., and Taichman, R. S. (2010) Erythropoietin couples hematopoiesis with bone formation, *PLoS One*, **5**, e10853.
3. Wu, C., Giaccia, A. J., and Rankin, E. B. (2014) Osteoblasts: a novel source of erythropoietin, *Curr. Osteoporos. Rep.*, **4**, 428-432.
4. Li, C., Shi, C., Kim, J., Chen, Y., Ni, S., Jiang, L., Zheng, C., Li, D., Hou, J., Taichman, R. S., and Sun, H. (2015) Erythropoietin promotes bone formation through EphrinB2/EphB4 signaling, *J. Dent. Res.*, **94**, 455-463.
5. Holstein, J. H., Menger, M. D., Scheuer, C., Meier, C., Culemann, U., Wirbel, R. J., Garcia, P., and Pohlemann, T. (2007) Erythropoietin (EPO): EPO-receptor signaling improves early endochondral ossification and mechanical strength in fracture healing, *Life Sci.*, **80**, 893-900.
6. Holstein, J. H., Orth, M., Scheuer, C., Tami, A., Becker, S. C., Garcia, P., Histing, T., Morsdorf, P., Klein, M., Pohlemann, T., and Menger, M. D. (2011) Erythropoietin stimulates bone formation, cell proliferation, and angiogenesis in a femoral segmental defect model in mice, *Bone*, **49**, 1037-1045.
7. Garcia, P., Speidel, V., Scheuer, C., Laschke, M. W., Holstein, J. H., Histing, T., Pohlemann, T., and Menger, M. D. (2011) Low dose erythropoietin stimulates bone healing in mice, *J. Orthop. Res.*, **29**, 165-172.
8. Rolfing, J. H. D., Bendtsen, M., Jensen, J., Stiehler, M., Foldager, C. B., Hellfritzsch, M. B., and Bunger, C. (2012) Erythropoietin augments bone formation in a rabbit pos-

terolateral spinal fusion model, *J. Orthop. Res.*, **30**, 1083-1088.
9. Sun, H., Jung, Y., Shiozawa, Y., Taichman, R. S., and Krebsbach, P. H. (2012) Erythropoietin modulates the structure of bone morphogenetic protein 2-engineered cranial bone, *Tissue Eng. Part A*, **18**, 2095-20105.
10. Rolfing, J. H., Jensen, J., Jensen, J. N., Greve, A. S., Lysdahl, H., Chen, M., Rejnmark, L., and Bunger, C. (2014) A single topical dose of erythropoietin applied on a collagen carrier enhances calvarial bone healing in pigs, *Acta Orthop.*, **85**, 201-209.
11. Patel, J. J., Modes, J. E., Flanagan, C. L., and Krebsbach, P. H. (2015) Dual delivery of EPO and BMP2 from a novel modular poly-ε-caprolactone construct to increase the bone formation in prefabricated bone flaps, *Tissue Eng. Part C Methods*, **21**, 889-897.
12. Omlor, G. W., Kleinschmidt, K., Gantz, S., Speicher, A., Guehring, T., and Richter, W. (2016) Increased bone formation in a rabbit long-bone defect model after single local and single systemic application of erythropoietin, *Acta Orthop.*, **87**, 425-431.
13. Wang, Y. J., Liu, Y. D., Chen, J., Hao, S. J., Hu, T., Ma, G. H., and Su, Z. G. (2010) Efficient preparation and PEGylation of recombinant human non-glycosylated erythropoietin expressed as inclusion body in *E. coli*, *Int. J. Pharm.*, **386**, 156-164.
14. Jeong, T. H., Son, Y. J., Ryu, H. B., Koo, B. K., Jeong, S. M., Hoang, P., Do, B. H., Song, J. A., Chong, S. H., Robinson, R. C., and Choe, H. (2014) Soluble expression and partial purification of recombinant human erythropoietin from *E. coli*, *Protein Expr. Purif.*, **95**, 211-218.
15. Boissel, J. P., Lee, W. R., Presnell, S. R., Cohen, F. E., and Bunn, H. F. (1993) Erythropoietin structure-function relationships. Mutant proteins that test a model of tertiary structure, *J. Biol. Chem.*, **268**, 5983-5993.
16. Narhi, L. O., Arakawa, T., Aoki, K., Wen, J., Elliott, S., Boone, T., and Cheetham, J. (2001) Asn to Lys mutations at three sites which are N-glycosylated in the mammalian protein decrease the aggregation of *Escherichia coli*-derived erythropoietin, *Protein Eng.*, **14**, 135-140.
17. Grunina, T. M., Demidenko, A. V., Lyaschuk, A. M., Poponova, M. S., Galushkina, Z. M., Soboleva, L. A., Cherepushkin, S. A., Polyakov, N. B., Grumov, D. A., Solovyev, A. I., Zhukhovitsky, V. G., Boksha, I. S., Subbotina, M. E., Gromov, A. V., Lunin, V. G., and Karyagina, A. S. (2017) Recombinant human erythropoietin with additional processable protein domains: purification of protein synthesized in *Escherichia coli* heterologous expression system, *Biochemistry (Moscow)*, **82**, 1285-1294.
18. Karyagina, A. S., Grunina, T. M., Poponova, M. S., Orlova, P. A., Manskikh, V. N., Demidenko, A. V., Strukova, N. V., Manukhina, M. S., Lyaschuk, A. M., Galushkina, Z. M., Cherepushkin, S. A., Polyakov, N. B., Solovyev, A. I., Zhukhovitsky, V. G., Tretyak, D. A., Boksha, I. S., Gromov, A. V., and Lunin, V. G. (2017) Synthesis in *Escherichia coli* and characterization of human recombinant erythropoietin with additional heparin-binding domain, *Biochemistry (Moscow)*, **83**, 1504-1522.
19. McCullough, P. A., Barnhart, H. X., Inrig, J. K., Reddan, D., Sapp, S., Patel, U. D., Singh, A. K., Szczech, L. A., and Califf, R. M. (2013) Cardiovascular toxicity of epoetin-alfa in patients with chronic kidney disease, *Am. J. Nephrol.*, **37**, 549-558.
20. Douros, A., Jobski, K., Kollhorst, B., Schink, T., and Garbe, E. (2016) Risk of venous thromboembolism in cancer patients treated with epoetins or blood transfusions, *Br. J. Clin. Pharmacol.*, **82**, 839-848.
21. Ruppert, R., Hoffmann, E., and Sebald, W. (1996) Human bone morphogenetic protein 2 contains a heparin-binding site, which modifies its biological activity, *Eur. J. Biochem.*, **237**, 295-302.
22. Karyagina, A. S., Boksha, I. S., Grunina, T. M., Demidenko, A. V., Poponova, M. S., Sergienko, O. V., Lyaschuk, A. M., Galushkina, Z. M., Soboleva, L. A., Osidak, E. O., Semikhin, A. S., Gromov, A. V., and Lunin, V. G. (2016) Optimization of rhBMP-2 active-form production in a heterologous expression system using microbiological and molecular genetic approaches, *Mol. Genet. Microbiol. Virol.*, **31**, 208-213.
23. Bartov, M. S., Gromov, A. V., Poponova, M. S., Savina, D. M., Nikitin, K. E., Grunina, T. M., Manskikh, V. N., Gra, O. A., Lunin, V. G., Karyagina, A. S., and Gintsburg, A. L. (2016) Modern approaches to research of new osteogenic biomaterials on the model of regeneration of cranial critical-sized defects in rats, *Bull. Exp. Biol. Med.*, **162**, 273-276.
24. Chen, X., Zaro, J. L., and Shen, W. C. (2013) Fusion protein linkers: property, design and functionality, *Adv. Drug. Deliv. Rev.*, **65**, 1357-1369.
25. Brines, M., Grasso, G., Fiordaliso, F., Sfacteria, A., Ghezzi, P., Fratelli, M., Latini, R., Xie, Q. W., Smart, J., Su-Rick, C. J., Pobre, E., Diaz, D., Gomez, D., Hand, C., Coleman, T., and Cerami, A. (2004) Erythropoietin mediates tissue protection through an erythropoietin and common beta-subunit heteroreceptor, *Proc. Natl. Acad. Sci. USA*, **101**, 14907-14912.
26. Rolfing, J., Baatrup, A., Stiehler, M., Jensen, J., Lysdahl, H., and Bunger, C. (2014) The osteogenic effect of erythropoietin on human mesenchymal stromal cells is dose-dependent and involves non-hematopoietic receptors and multiple intracellular signaling pathways, *Stem Cell Rev.*, **10**, 69-78.
27. Kim, J., Jung, Y., Sun, H., Joseph, J., Mishra, A., Shiozawa, Y., Wang, J., Krebsbach, P. H., and Taichman, R. S. (2012) Erythropoietin mediated bone formation is regulated by mTOR signaling, *J. Cell Biochem.*, **113**, 220-228.
28. Garcia, P., Speidel, V., Scheuer, C., Laschke, M. W., Holstein, J. H., Histing, T., Pohlemann, T., and Menger, M. D. (2011) Low dose erythropoietin stimulates bone healing in mice, *J. Orthop. Res.*, **29**, 165-172.
29. Holstein, J. H., Orth, M., Scheuer, C., Tami, A., Becker, S. C., Garcia, P., Histing, T., Morsdorf, P., Klein, M., Pohlemann, T., and Menger, M. D. (2011) Erythropoietin stimulates bone formation, cell proliferation, and angiogenesis in a femoral segmental defect model in mice, *Bone*, **49**, 1037-1045.
30. Li, C., Shi, C., Kim, J., Chen, Y., Ni, S., Jiang, L., Zheng, C., Li, D., Hou, J., Taichman, R. S., and Sun, H. (2015) Erythropoietin promotes bone formation through EphrinB2/EphB4 signaling, *J. Dent. Res.*, **94**, 455-463.
31. Karyagina, A. S., Boksha, I. S., Grunina, T. M., Demidenko, A. V., Poponova, M. S., Sergienko, O. V.,

Lyashchuk, A. M., Galushkina, Z. M., Soboleva, L. A., Osidak, E. O., Bartov, M. S., Gromov, A. V., and Lunin, V. G. (2017) Two variants of recombinant human bone morphogenetic protein 2 (rhBMP-2) with additional protein domains: synthesis in an *Escherichia coli* heterologous expression system, *Biochemistry (Moscow)*, **82**, 613-624.

32. Concepcion, J., Witte, K., Wartchow, C., Choo, S., Yao, D., Persson, H., Wei, J., Li, P., Heidecker, B., Ma, W., Varma, R., Zhao, L.-S., Perillat, D., Carricato, G., Recknor, M., Du, K., Ho, H., Ellis, T., Gamez, J., Howes, M., Phi-Wilson, J., Lockard, S., Zuk, R., and Tan, H. (2009) Label-free detection of biomolecular interactions using BioLayer interferometry for kinetic characterization, *Comb. Chem. High Throughput Screen.*, **12**, 791-800.
33. Gromov, A. V., Nikitin, K. E., Karpova, T. A., Zaitsev, V. V., Sidirova, E. I., Andreeva, E. V., Bartov, M. S., Mishina, D. M., Subbotina, M. E., Shevlyagina, N. V., Sergienkov, M. A., Soboleva, L. A., Kotnova, A. P., Sharapova, N. E., Semikhin, A. S., Didenko, L. V., Karyagina, A. S., and Lunin, V. G. (2012) Development of a method for preparation of osteoplastic material based on demineralized bone matrix with maximum content of native bone tissue growth factors, *Biotekhnologiya*, **5**, 66-75.
34. Heidenhain, M. (1905) Zeitschrift fur wissenschaftliche Mikroskopie und fur mikroskopische Technik, *S. Hirzel, Leipzig*, **22**, 339.
35. Zwingenberger, S., Langanke, R., Vater, C., Lee, G., Niederlohmann, E., Sensenschmidt, M., Jacobi, A., Bernhardt, R., Muders, M., Rammelt, S., Knaack, S., Gelinsky, M., Gunther, K. P., Goodman, S. B., and Stiehler, M. (2016) The effect of SDF-1α on low dose BMP-2 mediated bone regeneration by release from heparinized mineralized collagen type I matrix scaffolds in a murine critical size bone defect model, *J. Biomed. Mater. Res. A*, **104**, 2126-2134.
36. Hwang, C. J., Vaccaro, A. R., Lawrence, J. P., Hong, J., Schellekens, H., Alaoui-Ismaili, M. H., and Falb, D. (2009) Immunogenicity of bone morphogenetic proteins, *J. Neurosurg. Spine*, **10**, 443-451.